Agricultural and Forest Meteorology 221 (2016) 230–241

Contents lists available at ScienceDirect

Agricultural and Forest Meteorology

journal homepage: www.elsevier.com/locate/agrformet

# Influence of the decoupling degree on the estimation of canopy stomatal conductance for two broadleaf tree species

Zhen Z. Zhang[a,b], Ping Zhao[a,*], Heather R. McCarthy[c], Xiu H. Zhao[a,b], Jun F. Niu[a], Li W. Zhu[b], Guang Y. Ni[c], Lei Ouyang[a], Yu Q. Huang[d]

[a] Key Laboratory of Vegetation Restoration and Management of Degraded Ecosystems, South China Botanical Garden, Chinese Academy of Sciences, Guangzhou 510650, China
[b] University of Chinese, Academy of Sciences, Beijing 100049, China
[c] University of Oklahoma, Department of Microbiology and Plant Biology, Norman, OK 73019, USA
[d] Guangxi Institute of Botany, Chinese Academy of Sciences, Guilin 541006, China

ARTICLE INFO

*Article history:*
Received 11 September 2015
Received in revised form 18 January 2016
Accepted 25 February 2016
Available online 4 March 2016

*Keywords:*
Canopy stomatal conductance
Penman–Monteith equation
Monoculture plantations
Decoupling coefficient

ABSTRACT

Canopy stomatal conductance ($G_S$) estimation is a critical aspect of evapotranspiration research. Selecting an appropriate model for scaling-up is necessary to study plant water regulation. Two monoculture plantations of broadleaf tree species, *Eucalyptus urophylla* and *Schima superba,* were selected to study $G_S$ via a widely recognized equation simplified by Köstner ($G_{S1}$) and an inverse Penman–Monteith equation ($G_{S2}$). The decoupling coefficient ($\Omega$) was estimated to quantify the decoupling extent of stomata from the atmosphere. We found that both species were well coupled with environmental conditions ($0.1 \pm 0.06$ and $0.22 \pm 0.09$ for *E. urophylla* and *S. superba*). $\Omega$ increased exponentially with canopy conductance ($G_C$) and was depressed by the increase of $G_a$, which implied that there was a combined climatic and physiological regulation on $\Omega$. $G_{S1}$ for both species ($63.7 \pm 33.9$ mmol m$^{-2}$ s$^{-1}$ and $48.4 \pm 18.1$ mmol m$^{-2}$ s$^{-1}$ for *E. urophylla* and *S. superba,* respectively) was underestimated with the simplified equation compared to $G_{S2}$ ($77.0 \pm 52.4$ mmol m$^{-2}$ s$^{-1}$and $112.0 \pm 52.5$ mmol m$^{-2}$ s$^{-1}$ for *E. urophylla* and *S. superba*, respectively). The ratio of $G_{S1}/G_{S2}$ linearly decreased with $\Omega$ by a slope of $-1.92$ and $-1.31$ for *E. urophylla* and *S. superba*, respectively. The increase of the LAI tended to increase the decoupling extent, which further reduced the accuracy of the estimation of $G_{S1}$. According to our results, the ratio of $G_{S1}/G_{S2}$ had a mean of 0.94 for 85.3% and 0.6 for 37.6% of all of the data for *E. urophylla* and *S. superba*, respectively, implying a better estimation of $G_{S1}$ for the stand that had a lower LAI. Based on the relationship between the LAI and the ratios of $G_{S1}/G_{S2}$ (ratio = $1.0759 \times 0.02547^{(0.053\mathrm{LAI}+0.054)} - 0.0078$), we can shed some light on the prediction error of stomatal conductance derived from the simplified equation in different forest types.
© 2016 Elsevier B.V. All rights reserved.

## 1. Introduction

As one of the most important functional processes of forests for maintaining the water balance of catchments and regions, transpiration provides vital ecological services for social and economic activities (Huber et al., 2008; Little et al., 2009). Environmental changes will likely change this balance and force forests to make adjustments, resulting in corresponding variations in carbon assimilation. The environmental control of canopy transpiration can be characterized in terms of the response of canopy conductance to environmental factors (Kumagai et al., 2004, 2008; Barradas et al., 2005). Based on this, many studies relating canopy conductance to environmental factors have been conducted to explore the underlying mechanisms of such responses (Morris et al., 2006; Blanken and Black, 2004).

In 2013, the State Forestry Administration (SFA) reported that the forest area in China was 2.08 hundred million ha, covering 21.63% of the total land. Of this amount, planted forests consisted of 33.17% of the total forest area (6.9 million hectare), which is the largest area of plantations in the world (http://www.forestry.gov.cn/main/58/content-660036.html). *Eucalyptus urophylla*, one of the most common species introduced for afforestation in South China, has experienced rapid expansion over the past two decades and covered $1.65 \times 10^6$ ha in Guangxi (Forest Department of Guangxi

* Corresponding author.
*E-mail address:* zhaoping@scib.ac.cn (P. Zhao).

http://dx.doi.org/10.1016/j.agrformet.2016.02.018
0168-1923/© 2016 Elsevier B.V. All rights reserved.

Zhuang Autonomous Region, 2010, http://www.gxly.cn:8888/pub/cms/1/3545/3559/3566/88981.html). Because high productivity is often related with high rates of water use, there have been concerns that Eucalyptus planting will adversely affect water resources by reducing water yields from water-supply catchments (Whitehead and Beadle, 2004; Engel et al., 2005). With a large planting area and high water consumption, *E. urophylla* has been found to exert a significant impact on the regional hydrology and carbon assimilation (Lane et al., 2004). *Schima superb* is a native pioneer species in subtropical evergreen broad-leaf forests in South China, commonly used for reforestation in degraded hilly lands. Peng (1996) proposed a succession pathway from pioneer coniferous trees to shade intolerant broadleaf trees (such as *S. superba*) to shade tolerant broadleaf trees, based on field studies over several decades. Gao et al. (2003) argued that the fitness of a species for a particular succession stage at a particular location can be measured by stomatal behavior and biochemical assimilation capacity under local climate and soil conditions. Hence stomatal conductance response of *S. superba* to environmental changes played a vital role in forest succession.

Quantifying the environmental regulation of the transpiration of planted *E. urophylla* and *S. superba* forests is necessary and meaningful due to the significant environmental variability in subtropical South China, which is dominated by the monsoon climate. The application of sap flow techniques enabled the accurate estimation of tree transpiration and analyses on its interaction with abiotic factors at both individual and stand levels. According to Köstner et al. (1992), canopy conductance can be derived from sap flow measurements if the sap flow through the xylem changes as a consequence of the stomatal response to environmental variables. Thus, up-scaled sap flux may provide a convenient way to evaluate the effect of the environmental variability on stomatal conductance. The mean canopy stomatal conductance ($G_S$) can be estimated using sap flux measurements in representative trees in various forest stands. As proposed by Köstner et al. (1992):

$$G_S = (G_V T_a \rho E_L)/D \quad (1)$$

However, this approach is only valid when the following requirements are met: (1) water stored in the plant contributes little to transpiration compared to water uptake from soil; (2) there is no vertical pattern of D within the canopy; and (3) the leaf boundary layer conductance is much higher than the stomatal conductance (Aphalo and Jarvis, 1991), meaning that a canopy is considered to be well coupled to the atmosphere.

As noted by Schäfer et al. (2000), this method is justified for well-coupled tree species, such as conifers, whose leaf character and crown structure meet the above requirements. However, the application of this method in broadleaf forests is still limited by the leaf and canopy properties (Motzer et al., 2005; Zhao et al., 2006), primarily by large leaf sizes, which create a thick boundary layer around the surface of the leaves and forest canopy. As reported by Zhao et al. (2011) for *Acacia mangium*, the relatively broader leaves tended to be buffered from the ambient air by the boundary layer produced by transpiration, resulting in a gradual decrease of aerodynamic conductance. The contribution of stored water in the xylem to transpiration was also significant, accounting for 8–10% of the total daily transpiration. The lag between the basal sap flow and canopy transpiration in *A. mangium* was ~2 h in the dry season, suggesting a non-negligible resistance in the xylem. Lag times (2.5 h) have also been observed for *S. superba* in the dry season (Mei et al., 2010).

Despite its application limitations, Eq. (1) has been used in some research on canopy water regulation of broadleaf species (e.g., Ewers et al., 2007; Whitley et al., 2009), where a dimensionless decoupling coefficient (Ω) was calculated to analyze the dependence of canopy transpiration on physical or physiological factors. However, because Ω is not constant due to the temporal and spatial variance of the environmental conditions throughout a day, it may not be appropriate to apply Eq. (1) using an averaged value of Ω. Thus, there is a need to test whether a simple plant hydraulic model can capture the inherent features of $G_S$ with the daily and seasonal variability in Ω.

The Penman–Monteith equation (Monteith and Unsworth, 2007) is the most commonly used method to describe the process of canopy transpiration by integrating both plant physiology and micrometerological factors (Lu et al., 2003), and has frequently been applied to calculate a reference evapotranspiration ($ET_o$) index as a function of weather parameters. Its inverse form (Eq. (7)) is also widely applied to quantify canopy parameters (Zeppel and Eamus, 2008). This equation describes the relative importance of radiative and advective energy for the tree transpiration rate ($E_T$), the dominant evaporation component (Kelliher et al., 1992). This depends on the ratio of the aerodynamic to canopy conductances (Köstner et al., 1992). The model can be written as (Jarvis, 1976):

$$E_T = \Omega E_{eq} + (1 - \Omega) E_{imp} \quad (2)$$

where $E_{eq}$ is the transpiration rate obtained in equilibrium with an extensive, homogeneous wet surface via the energy balance, which is dominated by the airflow on the canopy. $E_{imp}$ is the transpiration rate imposed by the effects of the air saturation deficit (D, kPa). When Ω is small enough and $E_{eq}$ can be ignored, the $G_S$ estimation of Eq. (1) will be recovered from $E_{imp}$ (Köstner et al., 1992). Alternatively, the overestimated $E_{imp}$ would result in an overestimation of $G_S$. Therefore, we assume that the estimation of $G_S$ with Eq. (1) would be overestimated compared to the Penman-Monteith equation when applied to broadleaf species.

The objectives of this research were to: (1) evaluate the dynamic of the decoupling conditions of two planted forests, *E. urophylla* and *S. superba*, with similar environmental conditions throughout the year and (2) estimate the seasonal variation of stomatal control for the planted forests via two different methods and to compare their accuracy for the calculation of the canopy stomatal conductance in an attempt to acquire more accurate knowledge of stomatal conductance responses to environmental changes. We assumed that the simplified equation would underestimate $G_S$ for broad-leaf species because of its limitations. Based on this, we focused on the extent of the underestimation of the two broad-leaf species with different canopy structures, and aimed to determine the underlying mechanism of the underestimation among species based on the calculation of Ω.

## 2. Materials and methods

### 2.1. Site description

This study was conducted in separate *S. superba* and *E. urophylla* plantations. The *S. superba* plantation is situated in the South China Botanical Garden, Chinese Academy of Sciences, Guangdong Province, China (23°100′N, 113°210′E, altitude 41 m). It is characterized by a low subtropical monsoon climate, with an annual precipitation of 1612–1909 mm and a mean annual temperature of 21.4–21.9 °C. The wet season lasts from April to September, followed by the dry season, which lasts until the next March (Zhu et al., 2012). The *S. superba* stand was planted in the mid-1980s on a northeast-facing slope, with an inclination of 11.7°. The area contains a loam soil with a pH of 4.0, organic content of 2.3% and total nitrogen content of 0.07%. The *E. urophylla* plantation grows on a south-facing slope (inclination 28°) located at the Huangmian Forest Farm, Guangxi Province, China (24°78′N, 109°87′E). The *E. urophylla* experimental site is in the transitional zone between the low- and mid-subtropics, receiving abundant radiation and

**Table 1**
Stand parameters in the two experimental sites.[a]

| Species | Density | N | DBH | H | $A_S$ | LAI | $d_L$ | $A_L$ | Ac |
|---|---|---|---|---|---|---|---|---|---|
| *S. superba* | 603 | 21 | 15.5 (1.3) | 12.7 (0.5) | 0.018 (0.002) | 4.3 (0.1) | 9.1 (0.4) | 66.6 (10.2) | 20.7 (2.9) |
| *E. urophylla* | 1375 | 15 | 10.1 (0.6) | 11.5 (0.8) | 0.007 (0.001) | 1.5 (0.1) | 10.9 (0.2) | 21.0 (2.7) | 4.0 (0.2) |

[a] Density is the number of trees per hectare within the two sites, N is the number of sampled trees for sap flux monitoring, DBH is mean stem diameter at 1.3 m height (cm), H is mean tree height (m), $A_S$ is mean sapwood area ($m^2$), LAI is leaf area index ($m^2$ $m^2$), $d_L$ is mean leaf length (cm), Ac is mean crown size (East–West width times North–South width, $m^2$), and $A_L$ is tree level leaf area ($m^2$). Values in parentheses are standard deviations.

precipitation (1750–2000 mm) with an average annual temperature of 19–20.8 °C. The soil is dominated by krasnozem and upland yellowish red soil derived from malmstone and shale, with a pH of 3.5, organic content of 2.8% and total nitrogen content of 0.1%. The wet season begins in March, slightly earlier than that of the *S. superba* stand, and proceeds through August (Zhao et al., 2011). The dry season makes up the rest of the year. An instrument tower was installed in each plantation (18 m high for *S. superb* and 23.5 m high for *E urophylla*). The towers provided platforms for canopy parameter measurements (environmental conditions and sampling for leaf water potential determination) and environmental sensor installation. The *S. superb* stand had a denser canopy, with an average annual Leaf Area Index (LAI) of 4.33, while the LAI of the *E. urophylla* plantation was 1.53 (Table 1).

### 2.2. Sap flow

In order to choose the sample trees in each study, DBH of all trees in a 20m × 20 m plot within the two stands was measured, and trees were then divided into three groups based on their DBHs. Five to seven trees were randomly selected from each group, which lead to a sum of 15 and 21 individuals for *E. urophylla* and *S. superba*. Sap flux density ($F_d$, $gH_2O$ $m^{-2}$ $s^{-1}$) was measured with thermal dissipation probes (TDP) consisting of a heated (constant heat flow) probe and an unheated thermocouple probe. The probes were inserted into the wood xylem at breast height (1.3 m) on the north side of tree stems, as described by Granier (1987), Firstly, a small patch of bark (2 cm × 2 cm) was removed with a knife, and a hole of 20 mm in depth and 2.5 mm in width was drilled into the sap wood with an electric driller. Holes were filled with thermally conductive silicone before the sensors were installed. The upper probe was supplied with a constant power of 120 mA. The temperature difference between both probes was measured and converted to the sap flux density ($F_d$) (Granier, 1987). Data were read every 30 s and averaged and recorded every 10 min with a data logger (DL2e, Delta-T Devices, Ltd., Cambridge, UK). All sensors were covered with a plastic box and a piece of shading film to prevent the heating effect of sunlight during the daytime. Natural temperature gradients can influence sap flow measurements, with large potential errors. However, these effects were negligible in our study, since 98.5% and 97.1% of the temperature differences observed during periods of power failure fell below the threshold of 0.2 °C (Do and Rocheteau, 2002). Azimuthal variations of sap flow for *E. urophylla* were assumed to be negligible, since previous studies on these species (Zhou et al., 2004) have found no significant circumferential variation in sap flow (north, south, west and east, $p > 0.05$). Although we did not conduct circumferential measurements at the *S. superba* stand, circumferential measurements were made in another stand in Shimentai National Nature Reserve about 170 km from our stand, with *S. superba* as one of the studied species. No fixed pattern was observed, and the differences of sap flow for the four directions were non-significant (Fig. S1). Thus, we were justified in using one sap flow sensor per tree, given the insignificance and randomness of circumferential variations.

### 2.3. Environmental factors

Relative humidity and temperature were measured at the top of each tower (Model AV-S3 Temperature and Relative Humidity Probe) to calculate the vapor pressure deficit (D, kPa). During the study period, net radiation (Rn, W $m^{-2}$) was monitored with a net radiation sensor (NR2-07, UK), and soil heat flux (G, W $m^{-2}$) was measured with 3 soil heat flux plates (HFP01, Netherlands) buried 2 cm under the soil surface. Photosynthetic photon flux density ($Q_0$, μmol $m^{-2}$ $s^{-1}$) and solar radiation (W $m^{-2}$) above the canopy were separately measured with a quantum sensor (SKP 215, UK) and a pyranometer (SKS 1110), respectively, mounted next to each other. An anemograph (AN4-05, UK) was used to record the wind speed above the canopy. The soil water content (SWC, $m^3$ $m^{-3}$) was monitored with three soil moisture probes (SM300, UK) buried 30 cm under the ground surface. All of the environmental parameters were logged with the same reading frequency as the sap flow measurements and stored in another DL2e logger.

### 2.4. Stand parameters

We optically measured the LAI with a Li-Cor 2000 Plant Canopy Analyzer (Li-Cor, Lincoln, NE) every month. The stem diameter at breast height (DBH) of all of the sample trees was determined with a diameter tape, and the tree height (H) was measured with a clinometer (Sunto Tandem, Finland). The total leaf area of the sampled trees was obtained from the allometric relationship between DBH and the total leaf area based on trees harvested near the plots in 2009 (*S. superba*) and 2012 (*E. urophylla*). The stand parameters of the two sites are shown in Table 1. The stands differ in canopy parameters (LAI, tree level leaf area and crown size). *S. superba* and *E. urophylla* both have diffuse-porous wood, and the former possesses a much greater proportion of the sap wood area. An allometric equation relating the sapwood area ($A_S$) to diameter at the 1.3-m height (DBH) was developed from trees harvested outside the experimental sites and applied to the sampled trees. Sapwood depth and bark thickness were determined from the stem cores (5 mm in diameter) obtained with an increment borer from selected trees outside the sap flux measurement plots (5 m away, in the same stand, n = 10). Sapwood and heartwood were visually distinguished based on their color differences from dark yellow to light gray. Eqs. (3) and (4) show the $A_S$ relationships for *S. superba* and *E. urophylla*, respectively:

$$A_S = 00.0013 \times \exp(0.1526 \times \mathrm{DBH})(R^2 = 00.97) \quad (3)$$

$$A_S = 00.0012 \times \exp(0.1683 \times \mathrm{DBH})(R^2 = 00.96) \quad (4)$$

### 2.5. Canopy transpiration

Canopy leaf transpiration ($E_l$, kg $H_2O$ $m^{-2}$ $s^{-1}$) was derived from the sap flux density, leaf area and sapwood area. Many studies indicate the need for radial measurements of $F_d$ for appropriate tree and stand level scaling (Phillips et al., 1997; Ewers and Oren, 2000). Previous studies in *S. superba* showed that the sap flux density at a sapwood depth of 40–60 mm was 15% lower ($p < 0.0001$) than that of the outer 20 mm for, while sap flux at 0–20 mm and at 20–40 mm

showed no significant differences (Mei et al., 2010; Zhu et al., 2012). Therefore, $E_l$ for *S. superba* was calculated using the equation generated by Zhu et al. (2012), where the radial distribution of the sap flow was incorporated (Eq. (5)). In the case of *E. urophylla*, the sap wood depth (d) was 2.13 ± 0.40 cm, which was close to the length of the TDP probes. Therefore, the estimation of $E_l$ was derived from Eq. (6).

$$E_L = (F_d \times 00.85A_{S40} + F_d \times A_{S0\sim40})/A_L \quad (5)$$

$$E_L = F_d \times (A_S/A_L) \quad (6)$$

where $A_{s40}$ is the sapwood area at d > 40 mm and $A_{s0-40}$ is the sapwood area at 0 < d < 40 mm, $A_L$ refer to the total leaf area of tree individuals.

### 2.6. Canopy stomatal conductance

The simplified canopy stomatal conductance ($G_{S1}$, mmol $m^{-2}\,s^{-1}$) without considering aerodynamic resistance was estimated with Eq. (1). The combination of the inverse equation of Penman–Monteith (Kumagai et al., 2009) and the micrometerological data was used to evaluate canopy conductance ($G_C$, m $s^{-1}$) with the assumption of negligible understory transpiration and soil evaporation:

$$g_c = \frac{\gamma\lambda E_c g_a}{\Delta(R_n - G) + \rho c_p D g_a - \lambda(\Delta + \gamma)E_c} \quad (7)$$

where Δ: the slope of saturation vapor pressure vs. temperature relationship (kPa °$C^{-1}$); $R_n$: the net radiation absorbed by the canopy (MJ $m^{-2}\,h^{-1}$); G: the soil heat content absorbed by the ground (MJ $m^{-2}\,h^{-1}$); ρ: the density of dry air (kg $m^{-3}$); $c_p$: the specific heat of dry air at constant pressure (1.013 MJ $kg^{-1}$ °$C^{-1}$); D: the vapor pressure deficit (kPa); $G_a$: the aerodynamic conductance ($ms^{-1}$), as determined by Thom and Oliver (1977), which is presented in Eq. (8); $G_C$: the canopy conductance (mmol $m^{-2}\,s^{-1}$); λ: the latent heat of vaporization of water (2.45 MJ $kg^{-1}$); γ: the psychometric constant (0.0674 kPa °$C^{-1}$ at standard atmospheric pressure P = 101.3 kPa); and $E_c$: canopy transpiration ($E_l$, kg $m^{-2}\,s^{-1}$).

Canopy stomatal conductance ($G_{S2}$) is usually estimated from $G_C$ as:

$$G_S = \frac{g_c}{LAI_e} \quad (8)$$

where the effective leaf area index, $LAI_e$, can be set as the actual LAI for LAI ≤ 2, 2 for 2 < LAI < 4 and LAI/2 for LAI ≥ 4 (Qiu et al., 2013).

$G_a$ was estimated from wind speed as (Yunusa et al., 2000):

$$g_a = \frac{1 + 00.54u}{40.72(\ln(\frac{z}{z_0}))^2} \quad (9)$$

where z is the height at which wind velocity was measured (23.5 and 18.0 m for *E. urophylla* and *S. superba* stands), $z_o$ is the roughness height (0.123H, m), and U is the vertically averaged wind speed (m $s^{-1}$) within the canopy (m $s^{-1}$) estimate based on the U and LAI profiles within the canopy.

$$u = \frac{\sum_{h=1}^{H} U(h)}{\sum_{h=1}^{H} LAI(h)} \quad (10)$$

where U(h) and LAI(h) are the U and LAI at a height h within the canopy and H is the canopy height (m). Yi et al. (2008) found that for canopies with a uniform vertical distribution of the LAI, the momentum transfer through the canopy can be expressed by the following formula:

$$U(h) = u_0 e^{00.5LAI(h)((h/H)-1)} \quad (11)$$

where $u_0$ is the U at the top of the canopy and *a* is an attenuation coefficient (assumed to be 2.5) (Kim et al., 2014). The LAI profile was estimated from measurements at 2 m intervals from 1 m to 18 m and 23.5 m at the two sites (*S. superba* and *E. urophylla* stands respectively) along the towers, using an optical plant canopy analyzer (LAI-2000, LI-COR, Lincoln, NE, USA).

For a wide range of the zero plane displacement height, d (m) and the roughness length governing momentum transfer, $z_{om}$ (m) can be estimated from the canopy height H (m) by the following equations:

$$d = 2/3H \quad (12)$$

$$z_{om} = 0.123H \quad (13)$$

$$z_{oh} = 0.1z_{om} \quad (14)$$

In this study, $G_S$ was calculated after excluding data from the time periods when D < 100 Pa, and all of the units of conductance with m $s^{-1}$ were converted into mmol $m^{-2}\,s^{-1}$ by multiplying $4.16 \times 10^4$ (Pearcey et al., 2012).

### 2.7. Decoupling coefficient

The extent of canopy decoupling from the atmosphere can be described by a dimensionless coefficient that expresses the relative sensitivity of canopy transpiration to a marginal change in stomatal conductance (Jarvis and McNaughton, 1986):

$$\Omega = \frac{1}{1 + \left(\frac{\gamma}{\Delta+\gamma}\right)\left(G_a/G_C\right)} \quad (15)$$

### 2.8. Statistical analyses

The MIXED procedure was used to account for the effect of the time series data on the ANOVA calculations, as sap flux measurements often violated the assumption of independent errors, according to Ewers et al. (2007). Multiple regression analysis was conducted to test the dependence of Ω in $G_a$ and $G_C$, based on the estimation of standardized regression coefficient. Statistical analyses were performed using SAS (version 9.2, SAS Institute, Cary, NC). Origin pro (version 8.6, OriginLab, USA) was used to draw all of the graphs in the context.

## 3. Results

### 3.1. Environmental conditions during the period of sap flow measurements

$Q_0$ in the *E. urophylla* and *S. superba* forests had a mean of 422.9 ± 268.2 μmol $m^{-2}\,s^{-1}$ and 654.3 ± 274.9 μmol $m^{-2}\,s^{-1}$, respectively. Accordingly, the averaged daily D was 0.84 ± 0.63 kPa and 1.11 ± 0.66 kPa. Both stands had similar temperature variations throughout the year, with a mean of 22.18 °C and 22.54 °C for the *E. urophylla* and *S. superba* stands, respectively. The rainfall in the two stands was 1993.2 mm (*E. urophylla*) and 1632.3 (*S. superba*) mm, and it was mainly distributed between April and August (accounted for 75.1% and 79.1%, respectively), which is considered the wet season. Consistent with the rainfall patterns, mean SWC in the *E. urophylla* stand was higher (0.33 ± 0.06 $m^3\,m^{-3}$) than in the *S. superba* stand (0.28 ± 0.07 $m^3\,m^{-3}$). Growing on hillsides, the *E. urophylla* and *S. superba* stand experienced average wind speeds (*u*) of 1.42 ± 0.67 m $s^{-1}$ and 0.93 ± 0.56 m $s^{-1}$. Additionally, the wind speed (u, m $s^{-1}$) varied greatly among consecutive days, especially for *E. urophylla*.

### 3.2. Seasonal variation of the aerodynamic conductance and decoupling coefficient

The daily mean of $G_a$ was $2657.0 \pm 305.4$ and $2244.4 \pm 142.2$ mmol m$^{-2}$ s$^{-1}$ for *E. urophylla* and *S. superba*, respectively (Fig. 2a). In the *E. urophylla* stand, $G_a$ increased gradually from January, peaked in May, remained high until July, and then started decreasing. This type of unimodal curve was not observed in the *S. superba* stand. The coefficient of variability (CV) was 0.11 and 0.06 for *E. urophylla* and *S. superba*, respectively. The daylight hours average of Ω during the experiments (whole year) was $0.1 \pm 0.06$ (maximum = 0.45) and $0.22 \pm 0.09$ (maximum = 0.44) for *E. urophylla* and *S. superba*, respectively. The day-to-day variation of Ω showed a similar pattern for the two species, both of which peaked in the wet season (DOY 130 and 210 for *E. urophylla* and *S. superba* respectively).

### 3.3. Microclimatic control of decoupling coefficient

The atmospheric effect on Ω is a combined interaction of various environmental conditions, and thus, any individual role may be obscured by the others (Mielke et al., 1999). However, none of these variables alone can alter the Ω. According to Eq. (9), $G_a$ and $G_C$ were directly related with the change of Ω. A multiple regression analysis was conducted on the hourly data of $G_a$ and $G_C$ in relation to Ω. The standardized regression coefficient of $G_a$ and $G_C$ (−0.14 and 0.91, respectively, for *E. urophylla*, −0.02 and 0.96, respectively, for *S. superba*) showed the dominance of $G_C$ in explaining changes in Ω, with an exponential relationship between them (Fig. 3). Ω eventually approaches a maximum at a specific $G_a$ level. In addition, it seemed that the max Ω was limited by the range of $G_a$. When Ω=0.2 for the *E. urophylla* stand, $G_C$ reached 134.1, 176.7, 226.4 and 639.0 mmol m$^{-2}$ s$^{-1}$ at four different $G_a$ levels, i.e., the increased $G_a$ led to a larger canopy conductance under the given decoupling extent. A similar situation was also observed in the *S. superba* stand (Fig. 3b), contributing to a feedback inhibition on vapor movement from canopy to atmosphere.

### 3.4. The ratio of $G_{S1}/G_{S2}$

The daily variations of $G_{S1}/G_{S2}$ and the hourly average of each stand in October are shown in Fig. 4a. It was assumed that the stomata were closed under the zero light condition in our analysis. As a result, all of the data were chosen based on $Q_0 > 0$. The maximum ratios for both stands (1.05 and 0.74 for *E. urophylla* and *S. superba*) occurred at 6:00 am and gradually decreased until 9:00 am when a minimum value (0.91–0.92 and 0.33–0.36) was reached, remained at this value for some time, and then increased again. The daily means were 0.95 and 0.44 for *E. urophylla* and *S. superba*, respectively. The day-to-day variation of the ratio is presented in Fig. 4b. Similar to the parameters in Fig. 2, a unimodal pattern was observed for *E. urophylla*. The maximum ratio occurred during DOY 180-120 when light, $T_a$, rainfall and $G_a$ reached the maximum (Fig. 1). Comparably, the ratio value for *S. superba* dropped slightly from DOY 1 and recovered to the original level after DOY 300. In addition, the day-to-day variation of the ratio was more scattered for *S. superba*. The mean ratio throughout the year for *E. urophylla* was much higher than that of *S. superba* (0.87 and 0.45,respectively, $p < 0.01$).

### 3.5. The comparison of $G_{S1}$ with $G_{S2}$ and driving force of their variation

The daily means of $G_{S1}$ and $G_{S2}$ were compared to analyze the difference in the two models (Fig. 5a). A linear regression (not shown) was conducted for both species. The slope of $G_{S1}$, as a function of $G_{S2}$, for *E. urophylla* and *S. superba* was 0.54 and 0.19, respectively. Nonlinear analysis indicated that $G_{S1}$ tended to stabilize as $G_{S2}$ increased. In the cross-comparison of $G_{S1}$ and $G_{S2}$, $G_{S2}$ explained 85.1% of the variance for *E. urophylla*, while it explained only 31.2% of the variance for *S. superba*. We partitioned the dataset by $G_{S2}$ into intervals of 40 mmol m$^{-2}$ s$^{-1}$ and found that the slopes of the linear regression decreased from 0.98 (0–40 mmol m$^{-2}$ s$^{-1}$) to 0.43 (>160 mmol m$^{-2}$ s$^{-1}$) for *E. urophylla*. When the $G_{S2}$ of *S. superba* was <40 mmol m$^{-2}$ s$^{-1}$, the slope was 0.95 and decreased to 0.27 rapidly after $G_{S2}$ > 40 mmol m$^{-2}$ s$^{-1}$. This result implied that the simplified models underestimated the stomatal conductance for both species when Eq. (7) was applied, and the underestimation was amplified as $G_S$ increased.

The ratio of $G_{S1}$ to $G_{S2}$ was derived from the data in Fig. 5a. Because their slopes were changing (Fig. 5a) as $G_S$ increased, we attempted to determine the driving force for the variances of $G_{S1}/G_{S2}$ with a multiple regression analysis. The parameters that were input into the inverse Penman–Monteith equation were chosen for the analysis. Of note, Ω was also considered because it captured most of the variance in the climatic parameters and stomatal regulation ($G_a$, $G_C$). Ω accounted for the greatest variance (56.5% and 42.7%) for *E. urophylla* and *S. superba*, respectively. Finally, the ratio was fit as a function of Ω, as shown in Fig. 5b, which revealed a more dramatic decrease of $G_{S1}/G_{S2}$ for *E. urophylla* as Ω increased. The ratio of $G_{S1}/G_{S2}$ for *E. urophylla* was significantly higher ($0.84 \pm 0.14$, $p < 0.01$) when compared to the ratio for *S. superba* ($0.46 \pm 0.17$), and this was consistent with Fig. 5a.

We divided the data of the hourly mean ratio of $G_{S1}/G_{S2}$ into small datasets by Ω (0–0.7), with an interval of 0.05 for both species. This showed that the frequency of the estimated $G_{S1}/G_{S2}$ derived in Fig. 5b for *E. urophylla* ranged from 0.0003 to 0.3, and gradually decreased as Ω increased. A logistic regression analysis was performed, and the results showed a rapid decrease of the frequency after Ω > 0.15. The frequency for *S. superba* decreased from the maximum value of 0.18 when Ω < 0.05 and gradually decreased as Ω increased. This result showed that 85.3% of the analyzed data fell into the range 0 < Ω < 0.15. Comparatively, no dramatic decrease was observed for *S. superba*, and a higher frequency of larger Ω was found instead. The increase of LAI tended to equalize the distribution of Ω. As shown in Fig. 6, higher proportions of lower Ω were observed for *E. urophylla* than for *S. superba*. The mean value of $G_{S1}/G_{S2}$ at different Ω levels is also presented in Fig. 6. It linearly decreased (99.9% of all of the data) from the maximum of 1.02–0.25 when 0 < Ω < 0.5 and averaged 0.94 when 0 < Ω < 0.15 for *E. urophylla*, which implied a good agreement between the two models. Similar to the frequency, the ratio for *S. superba* also gradually decreased with increasing Ω, from an average of 0.67 when 0 < Ω < 0.05 to the minimum of 0.12 when 0.65 < Ω < 0.7. The mean of the first three Ω levels, which accounted for 37.5% of all of the data, was 0.60, mirroring a poor prediction of stomatal conductance estimated from the simplified equation. The comparison between both species also indicated that the ratios may differ from each other even at the same Ω level (Figs. 5 and 6), which may be caused by a specific difference in the leaf architectures.

## 4. Discussion

### 4.1. Coupling conditions between the canopy and atmosphere of broad leaf species

Significant seasonal changes of Ω were observed in the two forests (Fig. 2). Canopy conductance is highly associated with environmental conditions at many temporal scales (Gutiérrez et al., 1994; Tognetti et al., 2009). In our study, the exponential relationship between Gc and Ω indicated the indirect environmental control of Ω via the plant physiological regulation (Fig. 3). Kumagai

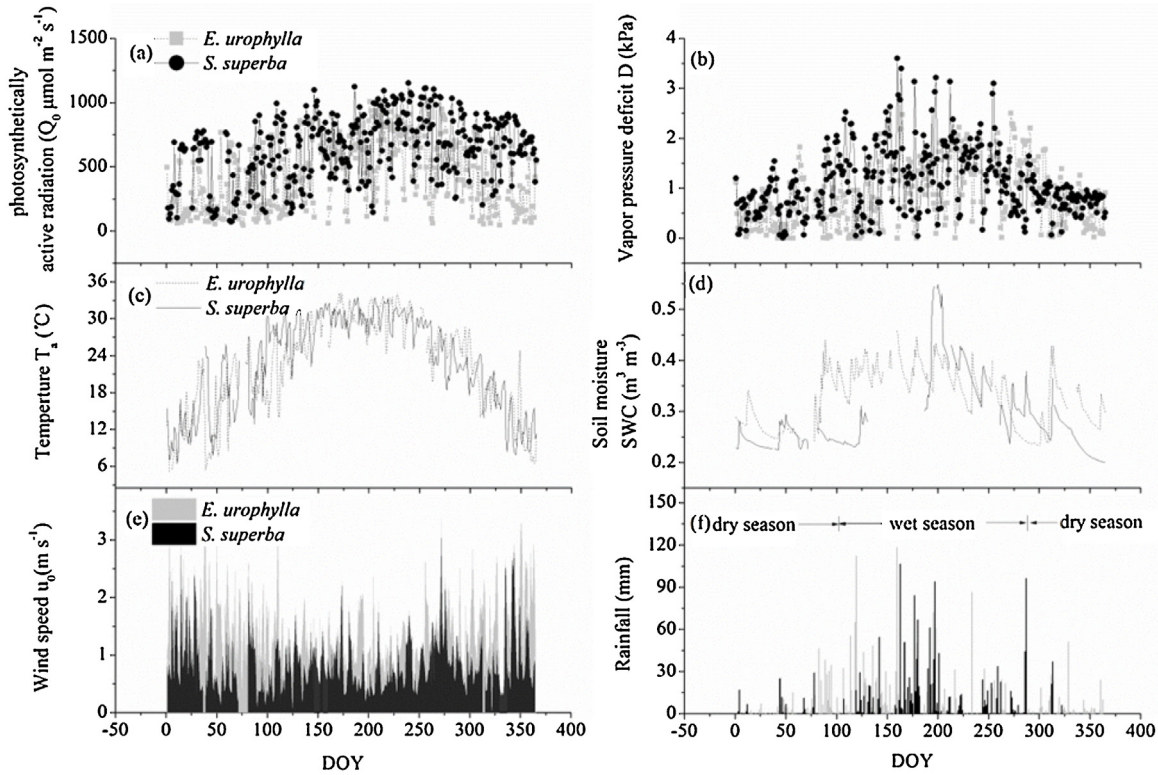


**Fig. 1.** Meteorological conditions during study periods: (a) photosynthetic photon flux density ($Q_0$); (b) vapor pressure deficit (D); (c) daily mean air temperature ($T_a$); (d) soil water content (SWC); (e) wind speed ($u_0$) above the canopy; (f) daily total rainfall in *E. urophylla* (June 2012–June 2013) and *S. superba* (in 2011) stands respectively. Missing data in the figures were due to instrument failure or power-down.

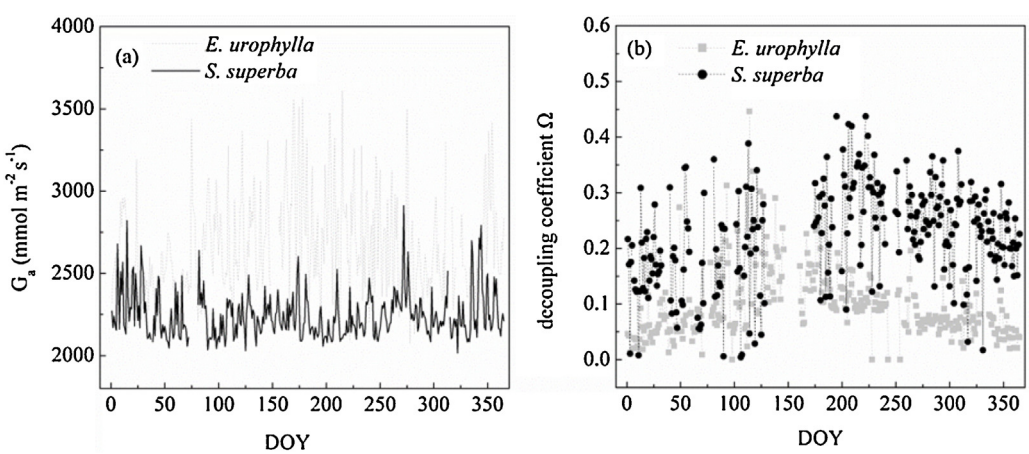


**Fig. 2.** Seasonal variation of aerodynamic conductance and decoupling coefficient Ω for the two stands over the course of the study.

et al. (2004) argued that the mean daily Ω was highly dependent on the soil moisture condition, which correlated with the seasonality in photosynthesis as a response of stomatal conductance. Cabral et al. (2010) found that the average Ω for *Eucalyptus* (*grandis* × *urophylla*) hybrid stands in the summer and winter was $0.6 \pm 0.08$ and $0.13 \pm 0.07$, respectively, with a similar density (1370 per hectare) to that of our *E. urophylla* stand and a LAI of 3.4 m$^2$ m$^{-2}$. They argued that intermediate Ω values were driven by the evaporation related to the seasonal changes of net radiation (Rn), the saturation deficit and, to some extent, the canopy conductance. The same results were also reported by Aires et al. (2008), who showed that the strong control of evapotranspiration by D dominated $G_S$ in the dry season. In addition to the indirect effect, Ω was also found to be related with environmental variables directly by changing $G_a$ of the canopy. As shown in Fig. 3, the higher $G_a$ allowed for a lower Ω at a given $G_C$.

In addition to the temporal regulation of environmental conditions, the structural difference between different forests also has substantial influences on the variation of Ω spatially. For example, even with a similar pattern of the seasonal fluctuation of Ω, the *E. urophylla* stand was better coupled than *S. superba,* which may be due to the lower LAI (Table 1). Consistently with this, Bracho et al. (2008) found a seasonal variation of Ω in response to the dynamic of the normalized difference vegetation index (NDVI) for scrub oak and pine flatwoods. The canopy resistance rose with the increasing LAI, which weakened the canopy-atmosphere coupling (Granier and Breda, 1996; Granier et al., 2000; Katsoulas et al., 2007) because the increase in the canopy leaf area may impede

**Table 2**
Summary of the literature that was used to obtain the relationship between leaf area index (LAI) and decoupling coefficient of different forest types across a variety of conditions.

| Species/forest type | Location | Rain (mm) | LAI ($m^2 m^{-2}$) | Ω | Methods | Authors |
|---|---|---|---|---|---|---|
| Mixed forest | | | | | | |
| Upland oak forest | Tennessee (America) | 716–1352 | 6.2 | 0.23 | TDP | Wullschleger et al. (2000) |
| Scrub oak | John F. Kennedy Space Center, florida (America) | 1237 ± 285 | 1.4 | 0.25 | Eddy Covariance | Bracho et al. (2008) |
| Lowland mixed dipterocarp forest | Lambir Hills National Park (Malaysia) | 2700 | 4.8–6.8 | 0.4 | Eddy Covariance | Kumagai et al. (2004) |
| *Elaeagnusangustifolia* L., *Populuseuphratica* Oliv., *and Ulmuspumila* L. | Khorezm (Uzbekistan) | 100 | 5 | 0.3 | Steady state porometer | Khamzina et al. (2009) |
| Siberian boreal forest | Lena River in eastern Siberia (Japan) | 259.2 | 1.6 | 0.1 | Steady state porometer | Iida et al. (2009) |
| Remnant woodland | Liverpool Plains (Australia) | 680 | 1–1.2 | 0.15 | Steady state porometer | Zeppel and Eamus (2008) |
| Black spruce forest | Poker Flat Research Range, Alaska (America) | 312 | 0.73 | 0.05 | Eddy Covariance | Nakai et al. (2013) |
| **Crops and grass** | | | | | | |
| Corn and soybeans | Miami (America) | – | 4 | 0.63–0.8 | Modeling | Gottschalck et al. (2000) |
| *Crotalaria juncea* L. | University of Tottori(Japan) | 1900 | 3.52 | 0.59 | Bowen Ratio | Takagi et al. (2009) |
| Rain-fed annual crops | Nalohou(Benin) | 1190 | 3 | 0.4 | Eddy Covariance | Mamadou et al. (2014) |
| *Phragmitesaustralis* | Panjin Wetland Ecosystem Research Station(China) | 630 | 3.8 | 0.45 | Eddy Covariance | Zhou et al. (2010) |
| Grass species | Inner Mongolia Grassland (China) | 320–400 | 1.7 | 0.1–0.5 | Eddy Covariance | Hao et al. (2007) |
| *Cynodondactylon* L. | Monte do Tojal, Evora (Portugal) | 364 | 2.5 | 0.39 ± 0.17 | Eddy Covariance | Aires et al. (2008) |
| Temperate grassland | Environmental Research Centre, University of Tsukuba (Japan) | 1300 | 5.5 | 0.55–0.8 | Eddy Covariance | Li et al. (2005) |
| **Pure forest** | | | | | | |
| *Fagus sylvatica* L. | Apennies (Italy) | – | 3.8 | 0.28 | Heat pulse | Magnani et al. (1998) |
| *Prosopis juliflora* | Biosaline Research Stations (Pakistan) | – | 1.8 | 0.15 | Heat pulse | Mahmood et al. (2001) |
| Banana | Zemach research station (Israel) | – | 4.3 | 0.3 | TDP | Liu et al. (2015) |
| *Acacia ampliceps* | | – | 6.7 | 0.4 | | |
| *Eucalyptus grandis* | Aracruz (Brazil) | 1400 | 3.8 | 0.25 | $CO_2/H_2O$ analyser | Mielke et al. (1999) |
| *Citrus limon*(L.) Burm fil. | Murcia (Spain) | – | 1.2 | 0.14 | Heat pulse | Nicolas et al. (2008) |
| *Quercuspetraea* | | | 4.2–6 | 0.1 | TDP | Granier and Bréda (1996) |
| *Quercusrobur* L. | | | 5.5 | 0.4 | Heated replica leaves | Stokes et al. (2006) |
| *Fagus crenata* Blume | Hokkaido lowlands (Japan) | | 7.5 | 0.5 | TDP | Tateishi et al. (2010) |
| | Honshu (Japan) | | 3.2 | 0.24 | | |
| | Kyushu Island (Japan) | | 2.8 | 0.15 | | |
| *Quercus ilex* L. | Presidential Estate of Castelporziano (Italy) | 753 | 3.68 | 0.22 | Ciras auto 1 | Vitale et al. (2003) |
| *Eucalyptus globulus* | Tasmania (Australia) | 515 | 8 | 0.63 | TDP | White et al. (2000) |
| *Pinussylvestris* L. | Huhus (Finland) | 724 | 1.98 | 0.14 | Eddy Covariance | Zha et al. (2013) |
| *Pinuscontorta var. latifolia* | British Columbia (Canada) | | 1.05 | 0.12 | Eddy Covariance | Brown et al. (2014) |
| *Prunusarmenica* L. | Murcia (Spain) | | 1 | 0.195 | Heat pulse | Barradas et al. (2005) |
| *Piceacrassifolia* | Guantan freeze/thaw observation station (China) | 435 | 1.5 | 0.08 | Eddy covariance | Zhu et al. (2014) |

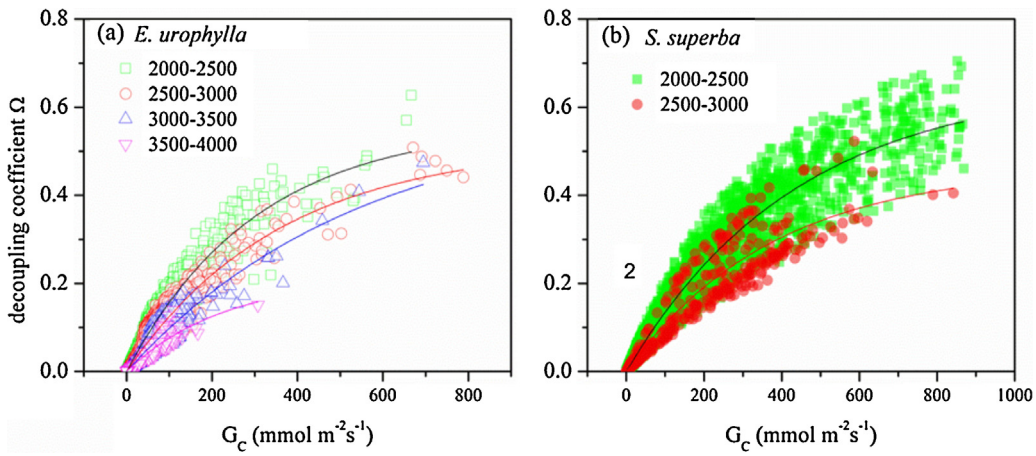


**Fig. 3.** Increasing decoupling coefficient (Ω) as a function of canopy conductance ($G_C$) at different aerodynamic conductances ($G_a$, mmol $m^{-2}$ $s^{-1}$) for the two stands. Lines are the exponential fit for each $G_a$ level.

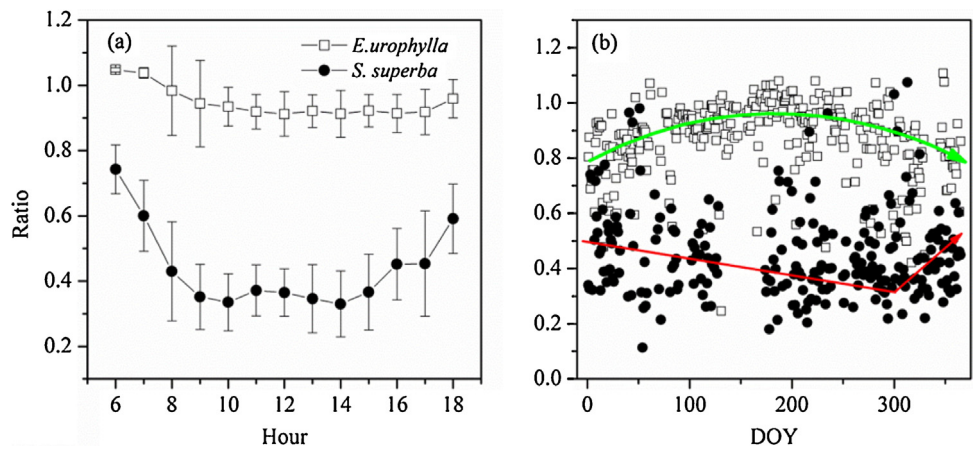


**Fig. 4.** (a) Daily course (Local Time) of $G_{S1}/G_{S2}$ ratio for the two stands in October, data are means ± SD, (b) day to day variation of the ratio during the study period. Arrows indicate the varying tendency of the ratio throughout the whole year.

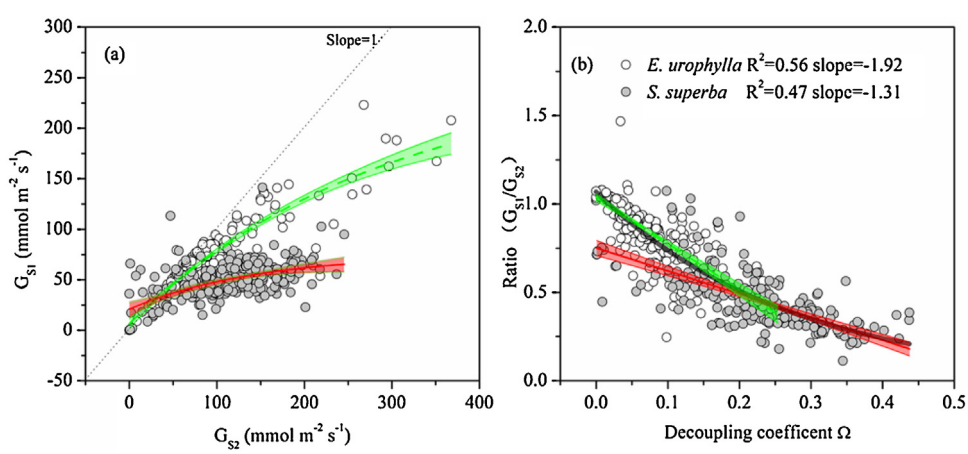


**Fig. 5.** (a) The daily integrated canopy stomatal conductance estimated from equation 1 ($G_{S1}$) versus that derived from the inverse Penmen–Monteith equation ($G_{S2}$) during the monitoring period when $Q_0 > 0$ μmol $m^{-2}$ $s^{-1}$; (b) The ratio of $G_{S1}$ to $G_{S2}$ as a function of decoupling coefficient Ω. Shaded areas represents the 95% confidence band for each curve-fit. Bold line is the exponential fit of all the data in the figure, ratio = $1.0759 \times 0.02547^{\Omega} - 0.0078$, $R^2 = 0.8$, $p < 0.01$.

air movement, decreasing $G_a$ while also decreasing D within the canopy (Kim et al., 2014). Even for the same species with similar density, Ω was higher for *Eucalyptus* stands with a more closed canopy (Cabral et al., 2010). Aiming to quantify the LAI control of Ω variance, we searched previous research that contained the LAI and decoupling coefficient of different forest types and grasses (Fig. 7b, Table 2) on the database "Web of Science" (https://apps.webofknowledge.com). As expected, all Ω of the three vegetation types (grasses, mixed forests, monoculture forests) followed the same pattern as the LAI increased. The mixed forest and

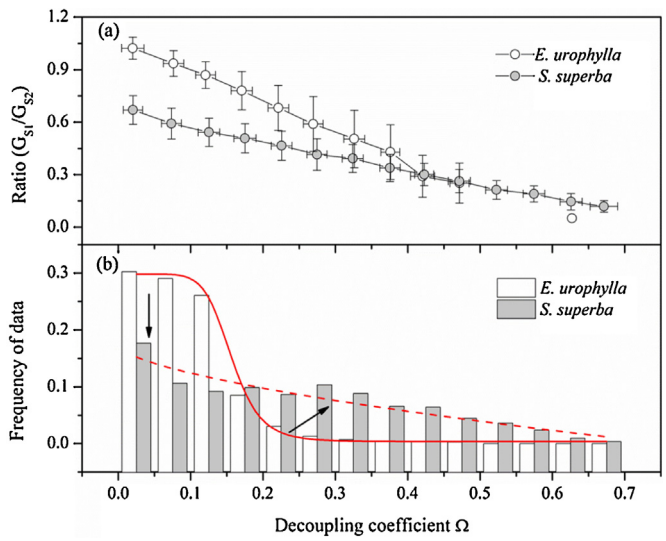


**Fig. 6.** (a) The integrated ratio of $G_{S1}$ to $G_{S2}$ (mean ± SD) at different decoupling coefficient (Ω) levels (at intervals of 0.05 from 0 to 0.7) and (b) the frequency of hourly data that was available for the estimation of stomatal conductance at decoupling coefficient (Ω) levels. Arrows indicates the changing tendency of frequency when LAI increases.

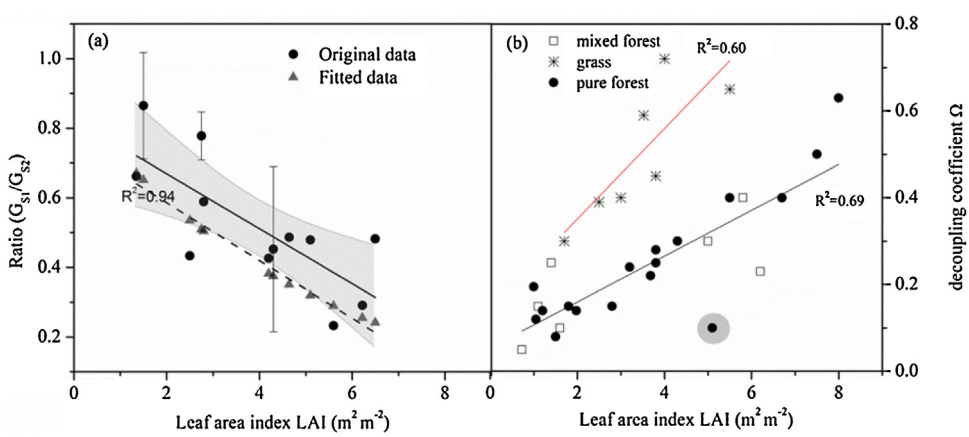


**Fig. 7.** (a) The relationship between leaf area index (LAI) and the ratio of $G_{S1}/G_{S2}$ and (b) LAI-dependent variation of decoupling coefficient (Ω) from literature and this study. Lines are the linear fit of each subset. Dotted line is the linear fit of predicted ratio from equation 11. Shaded area represents the 95 percent confidence band for the curve-fitting.

monoculture forests shared the same linear relationship, with a slope of 0.05, which was lower than that for grasses (0.1). This implied that the grass was more decoupled from the atmosphere at the same LAI, which may be caused by the lower wind speed on the ground. The results above indicate a complex decoupling relationship between broadleaf forests and atmospheric conditions, which are associated with the tree structure and the surrounding environmental conditions.

### 4.2. Underestimation of canopy stomatal conductance

Many studies have found that the inverse Penman-Monteith equation is a more accurate method for calculating forest transpiration (e.g., Yunusa et al., 2000; Pereira et al., 2006; Whitley et al., 2009). In our study, the slope of $G_{S1}$, as a function of $G_{S2}$, was 0.54 and 0.19 for *E. urophylla* and *S. superba*, respectively, demonstrating an underestimation of the stomatal conductance when Eq. (1) was applied. The $G_{S1}$ derived from Eq. (1) is the total water vapor conductance of the tree canopy (Köstner et al., 1992), which includes the stomatal ($G_S$), leaf boundary layer ($g_b$), and eddy diffusive conductance components ($G_a$), because it accounts for the conductance from the height of the "average" stomata in the tree canopy to the height of the measurement of D above the canopy (Thom, 1972). Significant errors may occur if the last two components are excluded for broad leaf species. Zhang et al. (1997) compared the predicted stomatal conductance estimated from the inverse Penman–Monteith equation with a combination equation proposed by Jarvis (1976), and showed an underestimate of $G_S$ at high values for the later. Another example of underestimation for the simplified equation was presented by Domec et al. (2009) when they compared $G_S$ with the leaf specific stomatal conductance. However, the extent of the underestimation seems to vary spatio-temporally.

The variation of LAI could be a key factor affecting the value of Ω and hence the estimation of the stomatal conductance on a spatial basis (Fig. 5b). We searched for studies that estimated $G_S$ via the inversed Penman–Monteith equation on the "Web of Science" database (https://apps.webofknowledge.com) and chose the parameters used to calculate $G_{S1}$ and then compared the ratio of $G_{S1}/G_{S2}$ (Table 3). We also chose the LAI of the studied forests from the literature and examined the relationship between LAI and the ratio of $G_{S1}/G_{S2}$ (Fig. 7a, Table 2). This showed that the increase of LAI correlated with a linear decrease of the ratio, i.e., the estimation of stomatal conductance would be underestimated more as the LAI increased. The ratio reached a minimum of 0.29 for the LAI = 6.22 for the upland oak forest studied by Wullschleger et al.

**Table 3**
Parameters that were used to estimate $G_{S1}/G_{S2}$ derived from the literature.We obtained all the data from the published graphs and tables. All of the units in the literature were converted into common units, as shown in the tables.

| Species/forests | LAI ($m^3\,m^{-3}$) | $G_{S2}$ ($mm\,s^{-1}$) | $E_L$ ($gm^{-2}\,s^{-1}$) | T (°C) | D (kPa) | $G_{S1}$ ($mm\,s^{-1}$) | $G_{S1}/G_{S2}$ | Authors | Resources |
|---|---|---|---|---|---|---|---|---|---|
| *Populus trichocarpa* × *P. tacamahaca* | 2.75 | 8.39 | 0.035 | 20.2 | 1.3 | 5.904782 | 0.703998 | Zhang et al. (1997) | Mid-day |
| | | 9.21 | 0.038 | 25.3 | 1.15 | 7.274596 | 0.789644 | | |
| | | 8.66 | 0.037 | 22.5 | 1.1 | 7.281739 | 0.840605 | | |
| Upland oak forest | 6.22 | 3.36 | 0.011 | 27.3 | 2.5 | 0.978285 | 0.29126 | Wullschleger et al. (2000) | Average |
| *Citrus sinensis* L. *Osbeck* | 4.64 | 3.67 | 0.008 | 25 | 1 | 1.78714 | 0.48662 | Oguntunde et al. (2006) | Fit function |
| Atlantic Forest | 5.1 | 2.2 | 0.004 | 18 | 0.9 | 1.053321 | 0.478782 | Pereira et al. (2010) | Average |
| Soybean | 6.5 | 3 | 0.008 | 20 | 1.2 | 1.446218 | 0.482073 | Mallick et al. (2013) | Fit function |
| Semi-deciduous tropical rainforest | 4.2 | 13.1 | 0.011 | 26.1 | 0.43935 | 5.544411 | 0.426493 | Sommer et al. (2002) | Average |
| Mixed beech/spruce stand | 5.6 | 4.28 | 0.013 | 30 | 3 | 0.994559 | 0.232374 | Nunn et al. (2010) | Mid-day |
| *Oleaeuropaea* L. | 2.5 | 7.68 | 0.027 | 10 | 1.7 | 3.327811 | 0.433309 | Tognetti et al. (2009) | Mid-day |
| *Oleaeuropaea* L. | 1.35 | 11.4 | 0.066 | 20.2 | 1.9 | 7.5407 | 0.661465 | Villalobos et al. (2000) | Mid-day |
| Mature poplar | 2.8 | 4.64 | 0.014 | 17 | 1.1 | 2.732692 | 0.588942 | Schmidt-Walter et al. (2014) | DOY210 |

(2000). Oren et al. (2001) noted that the assumption for the application of Eq. (1), which is that the leaf boundary layer conductance needs to be large relative to stomatal conductance, is satisfied for narrow leaf species, which turned out to be associated with the LAI in our research, since narrow leaf species tend to have a lower LAI. In this study, the ratios of $G_{S1}/G_{S2}$ had a mean of 0.94 (85.3% of all the *E. urophylla* data) and 0.6 for (37.6% of all the *S. superba* data) (Fig. 6), mirroring the limitation of the application of Eq. (1) as the LAI increased from 1.5 to 4.03. In addition, the other assumption of an even D distribution within the canopy also depend on LAI because a low LAI reduces the wind speed, which may further change the D profile within the canopy (Kim et al., 2014).

On a temporal basis, the ratio of $G_{S1}/G_{S2}$ varied significantly throughout the year, even over a single day (Fig. 4), because $G_a$ and $g_b$ (regulated by wind speed) constantly fluctuated (Figs. 1 e, 2 a). The high interpreting degree to the variance of $G_{S1}/G_{S2}$ (56.5% and 42.7%, respectively) for Ω indicated that the estimated deviation of the stomatal conductance ($G_{S1}$) was highly dependent on the variation of Ω (Fig. 4b). We combined the data of *E. urophylla* and *S. superba* in Fig. 5b, and a strong exponentially decreasing relationship was derived (Fig. 5b, $R^2 = 0.8$). While it is impractical to evaluate the underestimation of $G_S$ with the simplified equation via the calculation of Ω with Eqs. (7), (9) and (15) for all the forests, in most cases we only need to have knowledge of mean value of the underestimation. Fortunately, we found a relationship of Ω with LAI (Fig. 7b). We inferred that increasing LAI was prone to increase the decoupling extent and to distribute Ω more evenly among potential values (Fig. 6), which further amplified the error of the $G_{S1}$ estimation. Thus, Ω in the equation (ratio = 1.0759 × 0.02547 Ω − 0.0078) was replaced by the LAI based relationship of all of the forests in Fig. 7b, and a new equation was derived as:

$$\text{Ratio} = 1.0759 \times 0.02547^{(0.053\text{LAI}+0.054)} - 0.0078 \quad (16)$$

We predicted the ratio fit in Fig. 7a by the equation above, and a new linear relationship was obtained (Fig. 7a, dash line). This new relationship paralleled the original, with a decreasing (slope = −0.083) ratio with increasing, but lower values. One of the reasons for this result was that we chose the data when the $G_S$ reached its maximum values (around noon or during the growing season; Table 3), which would lead to a higher Ω (Fig. 3). However, most of the predicted dots fell into the 95% confidence band of the original fit. This implied that the new equation (Eq. (16)) associating the LAI with the ratio of $G_{S1}/G_{S2}$ was applicable to project the real stomatal conductance among forests with different degrees of closure, based on the simplified equation (Eq. (1)).

However, there are some concerns with the LAI-Ω data aggregation. Previous studies in forest ecosystem have reported a hysteresis between LAI and Gs. This might be related to the effects of environmental factors on stomatal aperture and/or the effects of leaf age on the decline in photosynthetic capacity (e.g., Wilson et al., 2000; Kitajima et al., 2002). The unbalanced LAI-Gs relationship may lead to variation of Ω around the LAI-Ω relation shown in Fig. 7b. This indeed happened in our analysis, since most points evenly scattered on both sides of fitted line in Fig. 7b (especially the shaded area, Table 2, Granier and Bréda, 1996). Although the LAI–Ω relationship is reasonable for most of the study if we consider the confidence interval (Fig. 7a), the established equation of Ω determined underestimation of $G_S$ associated with LAI is only an approximation of the real $G_S$ value. There are still many other variables that needed to be taken in consideration if we want to make $G_S$ estimation more accurate.

## 5. Conclusion

Seasonal dynamics of Ω were dominated by the variation in $G_C$ throughout the year and modified by the change of $G_a$, which mirrored a feedback inhibition on water movement from the forest canopy to the atmosphere. $G_{S1}$ (estimated with Eq. (1)) was underestimated when compared with $G_{S2}$ (estimated with Eq. (1)), especially for *S. superba*, which confirmed the hypothesis proposed in the Introduction. Temporally, the relationship between Ω and $G_{S1}/G_{S2}$ showed that Ω could be used to determine the degree of deviation of the stomatal estimation with the simplified equation (Eq. (1)). Spatially, the increase of the LAI altered the ratio by changing the Ω, which can be used to estimate the underestimation of stomatal conductance for different forests.

## Acknowledgement

This research Supported by the National Nature Science Foundation of China (41030638, 31170673, 41275169), the Provincial Nature Science Foundation of Guangdong (S2012020010933, 2014A030313762) and the CAS/SAFEA International Partnership Program for Creative Research Teams

## Appendix A. Supplementary data

Supplementary data associated with this article can be found, in the online version, at http://dx.doi.org/10.1016/j.agrformet.2016.02.018.

## References

Aires, L.M., Pio, C.A., Pereira, J.S., 2008. The effect of drought on energy and water vapour exchange above a mediterranean C3/C4 grassland in Southern Portugal. Agric. For. Meteorol. 148, 565–579.

Aphalo, P.J., Jarvis, P.G., 1991. Do stomata respond to relative humidity? Plant Cell Environ. 14, 127–132.
Barradas, V.L., Nicolas, E., Torrecillas, A., Alarcon, J.J., 2005. Transpiration and canopy conductance in young apricot (*Prunus armenica* L.) trees subjected to different PAR levels and water stress. Agric. Water Manage. 77, 323–333.
Blanken, P.D., Black, T.A., 2004. The canopy conductance of a boreal aspen forest, Prince Albert National Park, Canada. Hydrol. Process. 18, 1561–1578.
Bracho, R., Powell, T.L., Dore, S., Li, J., Hinkle, C.R., Drake, B.G., 2008. Environmental and biological controls on water and energy exchange in Florida scrub oak and pine flatwoods ecosystems. J. Geophys. Res.: Biogeosci. 113.
Brown, M.G., Black, T.A., Nesic, Z., Foord, V.N., Spittlehouse, D.L., Fredeen, A.L., Bowler, R., Grant, N.J., Burton, P.J., Trofymow, J.A., Lessard, D., Meyer, G., 2014. Evapotranspiration and canopy characteristics of two lodgepole pine stands following mountain pine beetle attack. Hydrol. Process. 28, 3326–3340.
Cabral, O.M.R., Rocha, H.R., Gash, J.H.C., Ligo, M.A.V., Freitas, H.C., Tatsch, J.D., 2010. The energy and water balance of a *Eucalyptus* plantation in southeast Brazil. J. Hydrol. 388, 208–216.
Do, F., Rocheteau, A., 2002. Influence of natural temperature gradients on measurements of xylem sap flow with thermal dissipation probes. 1. Field observations and possible remedies. Tree Physiol. 22, 641–648.
Domec, J.C., Noormets, A., King, J.S., Sun, G.E., McNulty, S.G., Gavazzi, M.J., Boggs, J.L., Treasure, E.A., 2009. Decoupling the influence of leaf and root hydraulic conductances on stomatal conductance and its sensitivity to vapour pressure deficit as soil dries in a drained loblolly pine plantation. Plant Cell Environ. 32, 980–991.
Engel, V., Jobbágy, E.G., Stieglitz, M., Williams, M., Jackson, R.B., 2005. Hydrological consequences of *Eucalyptus* afforestation in the Argentine Pampas. Water Resour. Res. 41 (W10409).
Ewers, B.E., Oren, R., 2000. Analyses of assumptions and errors in the calculation of stomatal conductance from sap flux measurements. Tree Physiol. 20, 579–589.
Ewers, B.E., Mackay, D.S., Samanta, S., 2007. Interannual consistency in canopy stomatal conductance control of leaf water potential across seven tree species. Tree Physiol. 27, 11–24.
Gao, Q., Peng, S.L., Zhao, P., Zeng, X.P., Cai, X.A., Yu, M., Shen, W.J., Liu, Y.H., 2003. Explanation of vegetation succession in subtropical southern China based on ecophysiological characteristics of plant species. Tree Physiol. 23, 641–648.
Gottschalck, J.C., Gillies, R.R., Carlson, T.N., 2000. The simulation of canopy transpiration under doubled $CO_2$: the evidence and impact of feedbacks on transpiration in two 1-D soil-vegetation-atmosphere-transfer models. Agric. For. Meteorol. 106, 1–21.
Granier, A., 1987. Evaluation of transpiration in a Douglas-fir stand by means of sap flow measurements. Tree Physiol. 3, 309–320.
Granier, A., Bréda, N., 1996. Modelling canopy conductance and stand transpiration of an oak forest from sap flow measurements. Ann. For. Sci. 53, 537–546.
Granier, A., Breda, N., 1996. Modelling canopy conductance and stand transpiration of an oak interannual variation in water vapor and energy exchange over a typical steppe in Inner Mongolia, China. Agric. For. Meteorol. 146, 57–69.
Granier, A., Loustau, D., Bréda, N., 2000. A generic model of forest canopy conductance dependent on climate, soil water availability and leaf area index. Ann. For. Sci. 57, 755–765.
Gutiérrez, M.V., Meinzer, F.C., Grantz, D.A., 1994. Regulation of transpiration in coffee hedgerows-covariation of environmental variables and apparent responses of stomata to wind and humidity. Plant Cell Environ. 17, 1305–1313.
Hao, Y., Wang, Y., Huang, X., Cui, X., Zhou, X., Wang, S., Niu, H., Jiang, G., 2007. Seasonal and interannual variation in water vapor and energy exchange over a typical steppe in Inner Mongolia, China. Agric. For. Meteorol. 146, 57–69.
Huber, A., Iroumé, A., Bathurst, J., 2008. Effect of *Pinus radiata* plantations on water balance in Chile. Hydrol. Process. 22, 142–148.
Iida, S.i., Ohta, T., Matsumoto, K., Nakai, T., Kuwada, T., Kononov, A.V., Maximov, T.C., van der Molen, M.K., Dolman, H., Tanaka, H., Yabuki, H., 2009. Evapotranspiration from understory vegetation in an eastern Siberian boreal larch forest. Agric. For. Meteorol. 149, 1129–1139.
Jarvis, P.G., 1976. The interpretation of the variations in leaf water potential and stomatal conductance found in canopies in the field. Philos. Trans. R. Soc. Lond. 273, 593–610.
Jarvis, P.G., McNaughton, K.G., 1986. Stomatal control of transpiration: scaling up from leaf to region. Adv. Ecol. Res. 15, 1–49.
Köstner, B.M.M., Schulze, E.-D., Kelliher, F.M., Hollinger, D.Y., Byers, J.N., Hunt, J.E., McSeveny, T.M., Meserth, R., Weir, P.L., 1992. Transpiration and canopy conductance in a pristine broad-leaved forest of Nothofagus: an analysis of xylem sap flow and eddy correlation measurements. Oecologia 91, 350–359.
Katsoulas, N., Baille, A., Kittas, C., 2007. Leaf boundary layer conductance in ventilated greenhouses: an experimental approach. Agric. For. Meteorol 144, 180–192.
Kelliher, F.M., Köstner, B.M.M., Schulze, E.-D., Hollinger, D.Y., Byers, J.N., Hunt, J.E., McSeveny, T.M., Meserth, R., Weir, P.L., 1992. Evaporation, xylem sap flow, and tree transpiration in a New Zealand broad-leaved forest. Agric. For. Meteorol. 62, 53–73.
Khamzina, A., Sommer, R., Lamers, J.P.A., Vlek, P.L.G., 2009. Transpiration and early growth of tree plantations established on degraded cropland over shallow saline groundwater table in northwest Uzbekistan. Agric. For. Meteorol. 149, 1865–1874.
Kim, D., Oren, R., Oishi, A.C., Hsieh, C.I., Phillips, N., Novick, K.A., Stoy, P.C., 2014. Sensitivity of stand transpiration to wind velocity in a mixed broadleaved deciduous forest. Agric. For. Meteorol. 192, 41–42.
Kitajima, K., Mulkey, S.S., Samaniego, M., Wright, S.J., 2002. Decline of photosynthetic capacity with leaf age and position in two tropical pioneer tree species. Am. J. Bot. 89 (12), 1925–1932.
Kumagai, T.O., Saitoh, T.M., Sato, Y., Morooka, T., Manfroi, O.J., Kuraji, K., Suzuki, M., 2004. Transpiration, canopy conductance and the decoupling coefficient of a lowland mixed dipterocarp forest in Sarawak, Borneo: dry spell effects. J. Hydrol. 287, 237–251.
Kumagai, T.O., Tateishi, M., Shimizu, T., Otsuki, K., 2008. Transpiration and canopy conductance at two slope positions in a Japanese cedar forest watershed. Agric. For. Meteorol. 148, 1444–1455.
Kumagai, T.O., Aoki, S., Otsuki, K., Utsumi, Y., 2009. Impact of stem water storage on diurnal estimates of whole-tree transpiration and canopy conductance from sap flow measurements in Japanese cedar and Japanese cypress trees. Hydrol. Process. 23, 2335–2344.
Lane, P.N., Morris, J., Ningnan, Z., Guangyi, Z., Guoyi, Z., Daping, X., 2004. Water balance of tropical eucalypt plantations in south–eastern China. Agr. For. Meteorol. 124, 253–267.
Li, S.G., Lai, C.T., Lee, G., Shimoda, S., Yokoyama, T., Higuchi, A., Oikawa, T., 2005. Evapotranspiration from a wet temperate grassland and its sensitivity to microenvironmental variables. Hydrol. Process. 19, 517–532.
Little, C., Lara, A., McPhee, J., Urrutia, R., 2009. Revealing the impact of forest exotic plantations on water yield in large scale watersheds in South-Central Chile. J. Hydrol. 374, 162–170.
Liu, H., Cohen, S., Lemcoff, J.H., Israeli, Y., Tanny, J., 2015. Sap flow, canopy conductance and microclimate in a banana screenhouse. Agric. For. Meteorol. 201, 165–175.
Lu, P., Yunusa, I.A., Walker, R.R., Müller, W.J., 2003. Regulation of canopy conductance and transpiration and their modelling in irrigated grapevines. Funct. Plant Biol. 30, 689–698.
Magnani, F., Leonardi, S., Tognetti, R., Grace, J., Borghetti, M., 1998. Modelling the surface conductance of a broad-leaf canopy: effects of partial decoupling from the atmosphere. Plant Cell Environ. 21, 867–879.
Mahmood, K., Morris, J., Collopy, J., Slavich, P., 2001. Groundwater uptake and sustainability of farm plantations on saline sites in Punjab province, Pakistan. Agric. Water Manage. 48, 1–20.
Mallick, K., Jarvis, A., Fisher, J.B., Tu, K.P., Boegh, E., Niyogi, D., 2013. Latent heat flux and canopy conductance based on Penman–Monteith, Priestley–Taylor equation, and Bouchet's complementary hypothesis. J. Hydrometeorol. 14, 419–442.
Mamadou, O., Cohard, J.M., Galle, S., Awanou, C.N., Diedhiou, A., Kounouhewa, B., Peugeot, C., 2014. Energy fluxes and surface characteristics over a cultivated area in Benin: daily and seasonal dynamics. Hydrol. Earth Syst. Sci. 18, 893–914.
Mei, T.T., Zhao, P., Wang, Q., Cai, X.A., Yu, M.H., Zhu, L.W., Zou, L., Zeng, X.P., 2010. Effects of tree diameter at breast height and soil moisture on transpiration of *Schima superba* based on sap flow pattern and normalization. Chin. J. Appl. Ecol. 21, 2457–2464 (in Chinese with English summary).
Mielke, M.S., Oliva, M.A., de Barros, N.F., Penchel, R.M., Martinez, C.A., de Almeida, A.C., 1999. Stomatal control of transpiration in the canopy of a clonal *Eucalyptus grandis* plantation. Trees Struct. Funct. 13, 152–160.
Monteith, J.L., Unsworth, M.H., 2007. Principles of Environmental Physics. Access Online via Elsevier.
Morris, J., Collopy, J., Mahmood, K., 2006. Canopy conductance and water use in *Eucalyptus* plantations. Pak. J. Bot. 38, 1485–1490.
Motzer, T., Munz, N., Küppers, M., Schmitt, D., Anhuf, D., 2005. Stomatal conductance, transpiration and sap flow of tropical montane rain forest trees in the southern Ecuadorian Andes. Tree Physiol. 25, 1283–1293.
Nakai, T., Kim, Y., Busey, R.C., Suzuki, R., Nagai, S., Kobayashi, H., Park, H., Sugiura, K., Ito, A., 2013. Characteristics of evapotranspiration from a permafrost black spruce forest in interior Alaska. Polar Sci. 7, 136–148.
Nicolas, E., Barradas, V.L., Ortuno, M.F., Navarro, A., Torrecillas, A., Alarcon, J.J., 2008. Environmental and stomatal control of transpiration, canopy conductance and decoupling coefficient in young lemon trees under shading net. Environ. Exp. Bot. 63, 200–206.
Nunn, A.J., Cieslik, S., Metzger, U., Wieser, G., Matyssek, R., 2010. Combining sap flow and eddy covariance approaches to derive stomatal and non-stomatal $O_3$ fluxes in a forest stand. Environ. Pollut. 158, 2014–2022.
Oguntunde, P.G., Friesen, J., van de Giesen, N., Savenije, H.H., 2006. Hydroclimatology of the volta river basin in west africa: trends and variability from 1901 to 2002. Phys. Chem. Earth 31, 1180–1188.
Oren, R., Sperry, J.S., Ewers, B.E., Pataki, D.E., Phillips, N., Megonigal, J.P., 2001. Sensitivity of mean canopy stomatal conductance to vapor pressure deficit in a flooded *Taxodium distichum* L. forest: hydraulic and non-hydraulic effects. Oecologia 126, 21–29.
Pearcey, R., Mooney, H.A., Rundel, P. (Eds.), 2012. Plant Physiological Ecology: Field Methods and Instrumentation. Springer Science and Business Media.
Peng, S., 1996. Southern Subtropical Forest Community Dynamics. Science Press China, Beijing, p. 444.
Pereira, A.R., Green, S., Nova, N.A.V., 2006. Penman–Monteith reference evapotranspiration adapted to estimate irrigated tree transpiration. Agric. Water Manage. 83, 153–161.
Pereira, D.D.R., de Mello, C.R., da Silva, A.M., Yanagi, S.D.N.M., 2010. Evapotranspiration and Estimation of Aerodynamic and Stomatal Conductance in a Fragment of Atlantic Forest in Mantiqueira Range Region, 16. MG, Cerne, Lavras, pp. 32–40.

Phillips, N., Nagchaudhuri, A., Oren, R., Katul, G., 1997. Time constant for water transport in loblolly pine trees estimated from time series of evaporative demand and stem sapflow. Trees 11, 412–419.
Qiu, R., Kang, S., Du, T., Tong, L., Hao, X., Chen, R., Chen, J., Li, F., 2013. Effect of convection on the Penman–Monteith model estimates of transpiration of hot pepper grown in solar greenhouse. Sci. Hortic.: Amsterdam 160, 163–171.
Schäfer, K.V.R., Oren, R., Tenhunen, J.D., 2000. The effect of tree height on crown level stomatal conductance. Plant Cell Environ. 23, 365–375.
Schmidt-Walter, P., Richter, F., Herbst, M., Schuldt, B., Lamersdorf, N.P., 2014. Transpiration and water use strategies of a young and a full-grown short rotation coppice differing in canopy cover and leaf area. Agric. For. Meteorol. 195, 165–178.
Sommer, R., Sa, T.D.D., Vielhauer, K., de Araujo, A.C., Folster, H., Vlek, P.L.G., 2002. Transpiration and canopy conductance of secondary vegetation in the eastern Amazon. Agric. For. Meteorol. 112, 103–121.
Stokes, V.J., Morecroft, M.D., Morison, J.I.L., 2006. Boundary layer conductance for contrasting leaf shapes in a deciduous broadleaved forest canopy. Agric. For. Meteorol. 139, 40–54.
Takagi, K., Kimura, R., Saylan, L., 2009. Variability of surface characteristics and energy flux patterns of sunn hemp (*Crotalaria juncea* L.) under well-watered conditions. Theor. Appl. Climatol. 96, 261–273.
Tateishi, M., Kumagai, T.O., Suyama, Y., Hiura, T., 2010. Differences in transpiration characteristics of Japanese beech trees, *Fagus crenata*, in Japan. Tree Physiol. 30, 748–760.
Thom, A.S., 1972. Momentum, mass and heat exchange of vegetation. Q. J. R. Meteorol. Soc. 98, 124–134.
Thom, A.S., Oliver, H.R., 1977. On Penman's equation for estimating regional evaporation. Q. J. R. Meteorol. Soc. 103, 345–357.
Tognetti, R., Giovannelli, A., Lavini, A., Morelli, G., Fragnito, F., d'Andria, R., 2009. Assessing environmental controls over conductances through the soil-plant-atmosphere continuum in an experimental olive tree plantation of southern Italy. Agric. For. Meteorol. 149, 1229–1243.
Villalobos, F.J., Orgaz, F., Testi, L., Fereres, E., 2000. Measurement and modeling of evapotranspiration of olive (*Olea europaea* L.) orchards. Eur. J. Agron. 13, 155–163.
Vitale, M., Scimone, M., Feoli, E., Manes, F., 2003. Modelling leaf gas exchanges to predict functional trends in Mediterranean *Quercus ilex* forest under climatic changes in temperature. Ecol. Model. 166, 123–134.
White, D.A., Beadle, C.L., Worledge, D., 2000. Control of transpiration in an irrigated *Eucalyptus globulus* Labill. plantation. Plant Cell Environ. 23, 123–134.
Whitehead, D., Beadle, C.L., 2004. Physiological regulation of productivity and water use in *Eucalyptus*: a review. For. Ecol. Manage. 193, 113–140.
Whitley, R., Medlyn, B., Zeppel, M., Macinnis-Ng, C., Eamus, D., 2009. Comparing the Penman–Monteith equation and a modified Jarvis–Stewart model with an artificial neural network to estimate stand-scale transpiration and canopy conductance. J. Hydrol. 373, 256–266.
Wilson, K.B., Baldocchi, D.D., Hanson, P.J., 2000. Quantifying stomatal and non-stomatal limitations to carbon assimilation resulting from leaf aging and drought in mature deciduous tree species. Tree Physiol. 20, 7787–7797.
Wullschleger, S.D., Wilson, K.B., Hanson, P.J., 2000. Environmental control of whole-plant transpiration, canopy conductance and estimates of the decoupling coefficient for large red maple trees. Agric. For. Meteorol. 104, 157–168.
Yunusa, I.A.M., Walker, R.R., Loveys, B.R., Blackmore, D.H., 2000. Determination of transpiration in irrigated grapevines: comparison of the heat-pulse technique with gravimetric and micrometeorological methods. Irrig. Sci. 20, 1–8.
Zeppel, M., Eamus, D., 2008. Coordination of leaf area, sapwood area and canopy conductance leads to species convergence of tree water use in a remnant evergreen woodland. Aust. J. Bot. 56, 97–108.
Zha, T., Li, C., Kellomaki, S., Peltola, H., Wang, K.-Y., Zhang, Y., 2013. Controls of evapotranspiration and $CO_2$ fluxes from scots pine by surface conductance and abiotic factors. PLoS One 8.
Zhang, H., Simmonds, L.P., Morison, J.I., Payne, D., 1997. Estimation of transpiration by single trees: comparison of sap flow measurements with a combination equation. Agric. For. Meteorol. 87, 155–169.
Zhao, P., Rao, X.Q., Ma, L., Cai, X.A., Zeng, X.P., 2006. Responses of canopy stomatal conductance of *Acacia mangium* forest to environmental driving factors. Chin. J. Appl. Ecol. 17, 1149–1156 (in Chinese with English summary).
Zhao, H.R., Xia, B.C., Jiang, X.D., 2011. Characteristics of precipitation change in guilin last 50 years. J. Guilin Univ. Technol. 31, 202–206 (in Chinese with English summary).
Zhou, G.Y., Yin, G.C., Morris, J., Bai, J.Y., Chen, S.X., Chu, G.W., Zhang, N.N., 2004. Measured sap flow and estimated evapotranspiration of tropical *Eucalyptus urophylla* plantations in South China. Acta Bot. Sin.: English Edition 46, 202–210.
Zhou, L., Zhou, G., Liu, S., Sui, X., 2010. Seasonal contribution and interannual variation of evapotranspiration over a reed marsh (*Phragmites australis*) in Northeast China from 3-year eddy covariance data. Hydrol. Process. 24, 1039–1047.
Zhu, L.W., Zhao, P., Cai, X.A., Zeng, X.P., Ni, G.Y., Zhang, J.Y., Zou, L.L., Mei, T.T., Yu, M.H., 2012. Effects of sap velocity on the daytime increase of stem $CO_2$ efflux from stems of *Schima superba* trees. Trees Struct. Funct. 26, 535–542.
Zhu, G., Lu, L., Su, Y., Wang, X., Cui, X., Ma, J., He, J., Zhang, K., Li, C., 2014. Energy flux partitioning and evapotranspiration in a sub-alpine spruce forest ecosystem. Hydrol. Process. 28, 5093–5104.